# THE ROLE OF ZEBRAFISH (*DANIO RERIO)* METABOLISM IN INFLUENCING PHYSIOLOGICAL FITNESS UNDER METABOLIC STRESS

An Undergraduate Research Scholars Thesis

by

MIKEELEE BRINK

Submitted to the Undergraduate Research Scholars program at
Texas A&M University
in partial fulfillment of the requirements for the designation as an

UNDERGRADUATE RESEARCH SCHOLAR

Approved by Research Advisor: Dr. David Hala

May 2020

Major: Marine Biology

# TABLE OF CONTENTS

# ABSTRACT

The Role of Zebrafish (*Danio rerio*) Metabolism in Influencing Physiological Fitness Under Metabolic Stress

Mikeelee Brink
Department of Marine Biology
Texas A&M University

Research Advisor: Dr. David Hala
Department of Marine Biology
Texas A&M University

Metabolism involves a network of interconnected reactions, of which pathways are responsible for growth, renewal, and cellular maintenance. Environmental stress can pose challenges for the proper functioning of these pathways. This project integrates physiological and bioinformatics approaches to study how metabolic pathways are adjusted under stress in zebrafish (*Danio rerio*). Metabolic stress in zebrafish was induced by exposing embryo-larval life-stages of fish to 1 μM of the tricarboxylic acid (TCA) cycle inhibitor, CPI-613, for 20 days. Physiological effects on whole-fish were determined using respirometry to measure oxygen consumption rate (as a proxy for metabolic rate). The oxygen consumption rate of fish was measured on Days 5, 10, 15, and 20 of exposure. The analysis of the effects of exposure to CPI-613 on metabolic rate showed significant decrease in oxygen consumption after 5 days of exposure, followed by a gradual recovery of oxygen consumption rates by Day 20 of exposure (i.e. equivalent to the solvent control group of 0.01% DMSO). In addition, whole-genome transcriptomics, or RNA-sequencing (RNA-seq), analysis was also performed on embryo-larval

zebrafish sub-sampled on Day 5 and 20 of exposure. The comparison of gene expressions for selected genes for Day 5 vs. Day 20 of exposure showed no effects on the expression of genes belonging to the pyruvate dehydrogenase complex (PDHC). However, in contrast to the genes of the PDH enzyme complex, a statistically significant increase in expression of hypoxia inducible factor (HIF-1$\alpha$) genes was observed at Day 5 relative to Day 20. The increase in HIF-1$\alpha$ expression indicates an adaptive response whereby zebrafish are inducing the expression of a transcription factor that helps an organism to adapt to metabolic stress (such as low oxygen or TCA cycle disruption). Taken together, the results of this project show an adaptive metabolic response that manifests both at the transcriptome level (i.e. upregulation of gene expression), and physiological level (increase in respiration rate).

# DEDICATION

I would like to dedicate this thesis to my family, who has provided me with undying support throughout my academic career.

# ACKNOWLEDGMENTS

First, I would like to thank my Faculty Advisor, Dr. David Hala, for his invaluable guidance, time, and support throughout this journey. He has provided me with knowledge of research that I will take with me to graduate school and other future endeavors. Most importantly, he has bestowed upon me his contagious passion for science, which has not only lead to the completion of this project, but has also helped me choose my future career path.

I would also like to extend my gratitude to Patricia Faulkner for her time and effort dedicated to the experiments and data analysis of this study. She has taught me many laboratory skills and techniques, and committed much of her time in doing so. She has also been an extremely positive influence on my future goals.

Thanks also goes to Kristina Simons for assisting me throughout this project. This project could not have been completed without her effort and cooperation.

Additionally, I would like to thank Dr. Lene Petersen for providing updates and reminders about deadlines and opportunities. She personally kept me on track throughout the entirety of this project.

And lastly, thanks go to Amy Caton and Ayaka Asada for sharing their knowledge of writing. They provided writing guidance as well as emotional support throughout all stages of the writing process. I could not have completed the writing of this thesis without their endless encouragement.

# NOMENCLATURE

| | |
|---|---|
| ADP | Adenosine Diphosphate |
| ATP | Adenosine Triphosphate |
| $CaCl_2$ | Calcium chloride |
| $CaCO_3$ | Calcium Carbonate |
| $CO_2$ | Carbon Dioxide |
| DI | Deionized |
| DMSO | Dimethyl Sulfoxide |
| Dpf | Days post fertilization |
| ECE | Electrical and Computer Engineering |
| ETC | Electron Transport Chain |
| $FAD^+$ | Flavin adenine dinucleotide |
| g | Gram |
| HIF | Hypoxia Inducible Factor |
| $H_2O$ | Water |
| KCl | Potassium Chloride |
| $KH_2PO_4$ | Potassium Dihydrogen Phosphate |
| L | Liter |
| M | Molar |
| m | Milli |
| $MgO_2$/kg/min | Milligram of Oxygen per kilogram fish per minute |
| $MgSO_4.7H_2O$ | Magnesium Sulfate |

| | |
|---|---|
| NaCl | Sodium Chloride |
| $NAD^+$ | Nicotinamide Adenine Dinucleotide |
| $NaHCO_3$ | Sodium Bicarbonate |
| $Na_2HPO_4$ | Disodium Phosphate |
| PDH | Pyruvate Dehydrogenase |
| PDHC | Pyruvate Dehydrogenase Complex |
| PDK | Pyruvate Dehydrogenase Kinase |
| ppt | Parts per thousand |
| RNA | Ribonucleic Acid |
| RNA-seq | RNA-sequencing |
| SC | Solvent Control |
| TCA | Tricarboxylic Acid Cycle |
| °C | Degrees Celsius |
| µ | Micro |

# CHAPTER I

# INTRODUCTION

## Environmental Stress

Environmental changes are accelerating the rate of extinction. The rate of extinction has reached its highest in the last decade and for the first time ever is due to a single species, humans (Helfman et al., 2009, pp. 3-10). A study performed that attempted to map the human impact on the global oceans, published in 2008, suggested that no part of the global oceans' ecosystems are untouched by human influence (Halpern et al., 2008). Human produced toxic substances enter ecosystems and induce harmful effects on organisms, such as interference with developmental pathways. These pathway interferences can result in a decrease in organism survival and reproduction (Helfman et al., 2009, pp. 3-10). Major changes in climate factors disrupt processes involved in maintaining organismal homeostasis, which leads to a selection pressure for organisms to adapt physiologically (Evans and Heather, 2019). Organisms have been observed to adapt to stressors by upregulation and downregulation of specific genes. However, impacts at the molecular level are not well understood (Cline et al., 2020).

The climate poses a challenge on most ecosystems in several different ways, both physiologically and molecularly. Ocean warming causes a decrease in oxygen levels in the water. This change in marine chemistry leads to an effect known as hypoxia, or the condition where the rate of oxygen consumption exceeds the rate of oxygen replenishment (Gobler and Baumann, 2016). Hypoxia can have an effect on metabolism and cardiac activity (Jacob et al., 2002). Aquatic nitrogen pollution due to nutrient effluents have been shown to decrease growth, reproduction, and activity levels, as well as increase developmental deformities in some

organisms (Gomez Isaza et al., 2020). An increase in environmental temperatures can alter growing season length and accelerate flowering and maturation in plants (Fournier-Level et al., 2016). The ability to maintain homeostasis during these environmental changes is achieved through the cells transcriptional control, where levels of proteins and ribonucleic acid (RNA) are modified (Hackley and Schmid, 2019).

**Metabolism as an Indicator for Physiological Fitness**

Metabolism is the sum of total metabolic rate that takes place in an organism (Helfman et al., 2009, 57-74). Metabolism plays many different roles in an organism such as growth, renewal, and generation of building blocks for cell maintenance. The metabolic network consists of genes, enzymes, and metabolites which are regulated by different stimuli (Fernández-García et al., 2020). The totality of metabolic conversions can be viewed as a network of interconnected reactions. As a result, metabolic and physiological functions can be altered if metabolic networks are perturbed by genetic and/or environmental stress (Barabasi and Oltvai, 2004; Hood et al., 2004; Schadt et al., 2009). Therefore associating underlying metabolic network functions to an organism's phenotype is an essential step towards understanding an organism's adaptive potential under stress (Barabasi and Oltvai, 2004; Frazier et al., 2003; Hartwell et al., 1999; Smart et al., 2008).

Cells must regulate energy metabolism in order to maintain homeostasis by allosteric regulation of the metabolic network, interplay between the signaling pathways, and regulation of transcription factors (Eguchi and Nakayama, 2019; Mulukutla et al., 2016). Glucose is an important molecule generated through metabolism and is a source of carbon for biosynthesis and generation of energy (Mulukutla et al., 2016). Glucose consumption yields adenosine triphosphate (ATP), which provides energy for cellular reactions through hydrolysis of the

molecule's high-energy phosphate bonds (Veerappa and McClure, 2020; Zimorski et al., 2019). The energy from ATP is harnessed through glycolysis and the tricarboxylic acid cycle (TCA cycle) through substrate phosphorylation as well as oxidative phosphorylation through the electron transport chain (ETC) (Veerappa and McClure, 2020). The metabolic pathways of glycolysis, the TCA cycle, and ETC are all connected in order to produce ATP more efficiently (Eguchi et al., 2019).

*Glycolysis*

Glycolysis is the oxidation of glucose to pyruvate in the absence of oxygen (Bolaños, et al., 2010; Fernie et al., 2004) (Figure 1(a)). This process produces two ATP molecules per glucose molecule (Jiang, 2017). Along with the production of ATP, electrons are generated from the breakdown of glucose and passed to the cofactor nicotinamide adenine dinucleotide ($NAD^+$) to generate NADH. The intermediates generated through glycolysis can be used to generate biomass, such as nucleic acids, lipids, and proteins. Pyruvate, the end product of glycolysis, enters the TCA cycle as acetyl-CoA for further processing (Locasale, 2018). Glycolysis is connected to the TCA cycle by pyruvate dehydrogenase (PDH), which converts pyruvate to acetyl-CoA for entry into the TCA cycle (Anderson et al., 2018; Eguchi and Nakayama, 2019).

*TCA Cycle*

One of the major functions of the TCA cycle is to oxidize acetyl-CoA to $CO_2$. The other major function is to generate energy in the form of ATP (Ciccarone et al., 2017; Vuoristo et al., 2016). One molecule of pyruvate yields 15 ATP molecules, outcompeting the 2 ATP yielded from glycolysis (Fernie et al., 2004). In the presence of oxygen, acetyl-CoA enters the TCA cycle, where a series of redox reactions occur which produce high-energy electrons. These electrons are then passed on to $NAD^+$ and $FAD^+$ (Flavin adenine dinucleotide) to generate

NADH and $FADH_2$ respectively (Anderson et al., 2018) (Figure 1(a)). One turn of the cycle also produces 3 NADH molecules, and 1 $FADH_2$ molecule to be passed on to the electron transport chain (Evans and Heather, 2019).

*Electron Transport Chain*

The electron transport chain (ETC) is located in the mitochondrial cristae membrane (Cogliati et al., 2018). The ETC consists of protein complexes imbedded in the inner mitochondrial membrane. Electron transport is coupled with proton pumping. NADH and $FADH_2$ are oxidized, releasing $H^+$ into the ETC. The electrons passed along the ETC move down the energy gradient and are finally accepted by oxygen to form $H_2O$ making the process aerobic (Cogliati et al., 2018; Ciccarone et al., 2017). ATP synthase uses a proton gradient to generate ATP from adenosine diphosphate (ADP) via oxidative phosphorylation (Cogliati et al., 2018; Veerappa and McClure, 2020). The ETC is the final step in the aerobic conversion of glucose to ATP and results in 32 ATP for every glucose molecule catabolized (Enderle, 2012) (Figure 1(a)).

**CPI-613 as a TCA Cycle Inhibitor**

CPI-613 is an anticancer drug that is used to inhibit upregulated metabolism in tumor cells. It is referred to as an anti-mitochondrial agent due to its ability to inhibit mitochondrial function (Bellio et al., Egawa et al., 2018; 2019; Lee et al., 2014; Lycan et al., 2016; pardee et al., 2014). Several studies involving cell lines, animal models, and phase I and II clinical studies have assessed the mitochondrial function in tumor cells after being dosed with CPI-613. The studies found that CPI-613 disrupted tumor cell mitochondrial metabolism and growth (Egawa et al., 2018; Lee et al., 2014; Pardee et al., 2014; Stuart et al., 2014; Zachar et al., 2011).

CPI-613 alters metabolism by targeting the TCA cycle (Figure 1 (b)). The agent functions by inhibiting PDH, a catalyst of the pyruvate conversion to acetyl-CoA for entry into the TCA

cycle (Anderson et al., 2018; Bellio et al. 2019; Lee et al., 2014; Pardee et al., 2014; Pardee et al. 2018). The TCA cycle is important because it generates cellular energy and metabolic precursors, such as ATP, lipids, proteins, and nucleic acids in the form of aerobic metabolism (Anderson et al., 2018; Lee et al., 2014). CPI-613 is an effective anticancer drug because cancer cells rely heavily on these molecules produced by the TCA cycle (Anderson et al., 2018). Inhibiting the TCA cycle prevents the cell from metabolizing carbon, which is used for anabolism in the cell (Pardee et al., 2014; Zachar et al., 2011).

**Key Metabolic Enzymes**

PDH is a metabolic enzyme that connects Glycolysis to the TCA cycle (Figure 1(b)). PDH converts pyruvate, the end product of glycolysis, to acetyl-CoA for entry into the TCA cycle. The enzyme works as a protein complex (PDHC) consisting of five major subunits (Eguchi and Nakayama, 2019). The complex consists of three catalytic domains which are E1 (pyruvate decarboxylase) with $\alpha$ and $\beta$ subunits, E2 (dihydrolipoamide acetyltransferase), and E3 (dihydrolipoamide dehydrogenase) (Maj et al., 2006). PDHC is regulated by pyruvate dehydrogenase kinase (PDK). PDKs inactivate PDHCs by phosphorylation at the E1$\alpha$ subunit, which as a result stops the conversion of pyruvate to acetyl-coA. PDK1, PDK2, PDK3, and PDK4 are the specific sites responsible for phosphorylating PDHC. PDK downregulates the activity of PDHC, which increases the conversion of pyruvate to lactate (Jha et al., 2016).

Hypoxia has an impact on metabolism. Cells have evolved a way to maintain homeostasis during a decrease in oxygen content. Hypoxia inducible factors (HIF) are transcription factors used by cells in order to adapt to the effects of hypoxia. These transcription factors work by downregulating aerobic processes and upregulating anaerobic processes (Sousa Fialho et al.,

2019). Aerobic metabolic genes have been found to be down regulated in hypoxic conditions. HIF-1α promotes cellular response to reduced oxygen levels (Kwong et al., 2016).

**Metabolic Rate and Pathway Regulation**

Moving towards a quantitative framework to study and define an organism's adaptive potential requires the quantitative integration of biochemistry (i.e. metabolic pathways) with physiology (metabolic rate). At present, an aggregate property of 'metabolic rate' is used to represent overall physiological fitness. Metabolic rate in an organism is assessed by measuring oxygen consumption, whose availability constrains, or limits, the scope of aerobic activities, such as feeding, foraging or fecundity, that can be undertaken by an organism. From an ecological perspective, metabolic rate is a good proxy for phenotypic fitness. However, underlying biochemical pathways of aerobic and anaerobic metabolisms are also highly deterministic towards fitness (Dahlhoff, 2004). At the metabolic level, organisms are known to increase their chance of survival by utilizing redundant pathways which share the production of specific intermediates so that the removal of an enzyme will be less likely to prevent the organism from producing key components of metabolism (Burgard et al., 2003).

In this study, I am using CPI-613 to cause targeted metabolic disruption. This approach is unique from most studies which target widespread disruption, such as hypoxia (Cline et al., 2020). Instead I am specifically targeting the TCA cycle and identifying how specific systems are affected in turn. Organisms have the potential to adapt to certain stressors, and have been shown to do so by either upregulating or downregulating certain genes. However, impacts at the molecular level are not well understood (Cline et al., 2020). It is beneficial to understand how an organism will react at the molecular level, in order to predict the affects at the physiological level. I will be assessing the oxygen consumption rate and RNA counts of early life stage

zebrafish (*Danio rerio)*. The purpose of this experiment is to provide insight into how the regulation of metabolic pathways influences an organism's ability to cope with stress. My hypothesis is that the ability of an organism to divert its metabolism between aerobic and anaerobic metabolic pathways will confer an adaptive advantage while under stress.

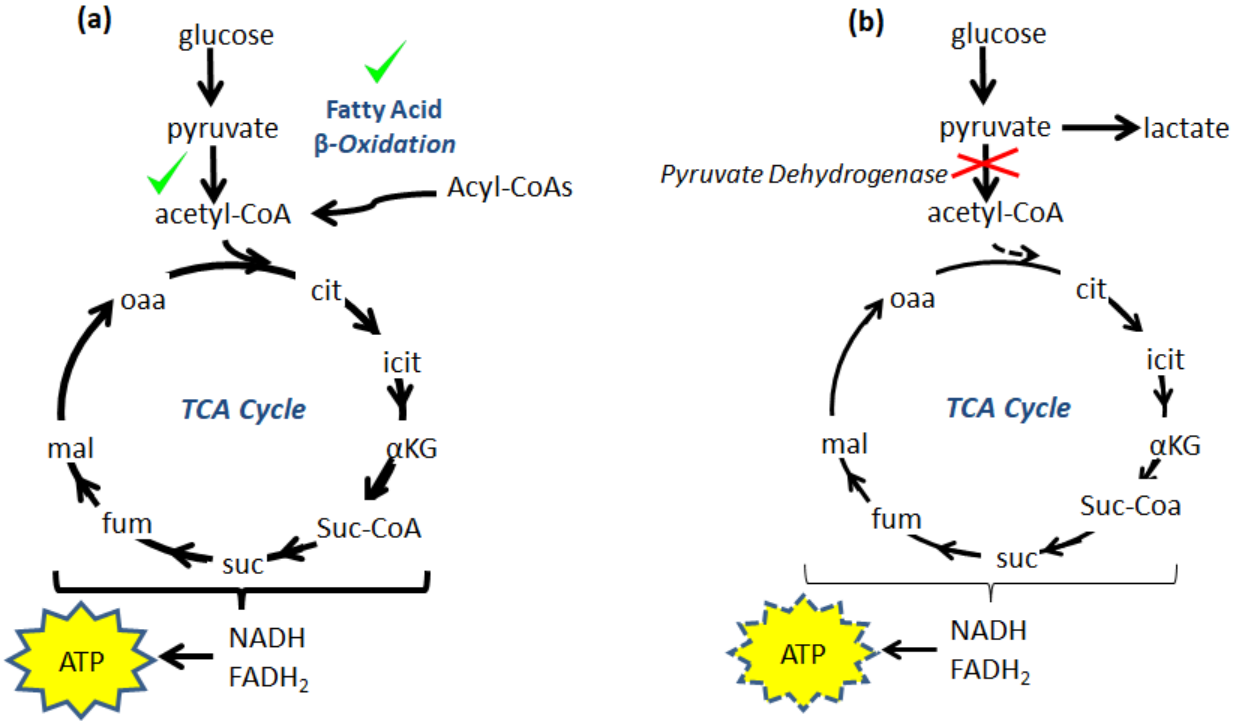


Figure 1. Abbreviated metabolic maps showing normal glucose metabolism via glycolysis, TCA cycle, and the electron transport chain (Generating ATP) (a); and the metabolic consequence of exposure to CPI-613, which inhibits pyruvate dehydrogenase, and lowering the activity of the TCA cycle (b).

Zebrafish were chosen as a model organism due to their well understood molecular biology and biochemistry as well as their common use as organisms in environmental quality assessment. Zebrafish are ideal for an in vivo study of developmental and reproductive toxicity to chemicals due to their rapid development (Haggard et al., 2016). A global transcriptomic

approach will be performed in order to identify the developmental affects from targeted metabolic stress and the mechanisms involved.

# CHAPTER II

# METHODS

## Zebrafish Husbandry

100 wild-type zebrafish embryos (*Danio rerio*) were purchased from the Zebrafish International Resource Center (ZIRC, Eugene, OR). 50 embryos were placed in petri dishes containing Embryo Medium from 0-4 days-post fertilization (dpf). The larval zebrafish were placed in 100 mL glass beakers containing culture water from 5-20 dpf. Both cultures were maintained at 28°C using a buffer tank. The larvae were cultured under semi-static renewal conditions, where 50% of the water was changed every 24 hours. The water was removed with a syphon along with any debris. The larval zebrafish were fed 150 μL of paramecia once daily starting at 5 dpf. At 11-20 dpf the zebrafish were fed 100-150 μL of AP 100-3 Zeiglar diet and 100-150 μL of brine shrimp.

Water parameters were checked once daily. The parameters and their optimum ranges can be found in Table 1. Test strips (LaMotte™, Insta-Test® 6-Way Drinking Water) were used to test the Nitrate, Nitrite, pH, and total Hardness. Also, test strips (LaMotte™, Insta-test® Analytic, Fresh and Salt Water) were used to test the ammonia. The pH was also tested using a pH meter (PC-700 Oaklon). Lastly, the salinity was measured using a salinity refractometer (Vital Sine™).

Table 1. Water parameters tested on the zebrafish culture water and their respective optimum range (Avdesh et al., 2012)

| **Parameters** | **Optimum Range** |
|---|---|
| Temperature | 26-28.5°C |
| pH | 6.8-7.5 |
| Hardness | 50-150 mg/L $CaCO_3$ |
| Un-ionized Ammonia ($NH_3$) | <0.02 mg/L |
| Nitrate ($NO_3^-$) | <50 mg/L |
| Nitrite ($NO_2^-$) | <0.1 mg/L |
| Dissolved Oxygen | >6.0 mg/L |
| Salinity | 0.5-1 g/L |
| Conductivity | 300-1500 μS |

**Embryo Medium**

From 0-4 dpf zebrafish were cultured in petri dishes using a 0.5 x E2 working solution of embryo medium. A 1 x E2 Embryo Medium was prepared by combining the compounds and quantities listed in Table 1 into 400 mL of filtered system water (Aqua FX reverse Osmosis system). Next, 16.6 μL of 0.1 % Methylene Blue was added to the solution. The embryo medium was brought to a pH of 7.2 using 1 M NaOH. 1 L of a 0.5xE2 Embryo Media was prepared by adding 500 mL of filtered system water to the solution. Then, the pH was adjusted back to 7.2. The culture was heated to 28°C before use.

Table 2. 1xE2 Embryo Medium components and their respective quantities.

| **Components** | **Quantity (g)** |
|---|---|
| 15 mM NaCl | 0.44 |
| 0.5 mM KCl | 0.02 |
| 1.0 mM $MgSO_4.7H_2O$ | 0.12 |
| 0.15 mM $KH_2PO_4$ (monobasic) | 0.01 |
| 0.05 mM $Na_2HPO_4$ (dibasic) | 0.004 |
| 1.0 mM $CaCl_2$ | 0.06 |
| 0.7 mM $NaHCO_3$ | 0.03 |

**Larvae Culture**

The zebrafish larval culture was prepared by combining 958 mL of filtered system water and 42 ml of 24 ppt in a 1 L volumetric flask to obtain a 1 g/L of salt in the final stock solution. For the treatment culture, CPI-613 was added to the volumetric flask to bring the concentration to 1 μM of CPI-613. For the solvent control (SC) group DMSO was added to bring the concentration to 0.01% DMSO. Two trials were performed exposing zebrafish to CPI-613 (treatment group) and DMSO (SC group). The drug stability of CPI-613 was tested throughout the trial using analytical mass spectrometry.

**Paramecia Culture**

The seed culture was made by adding 1 pellet of brewer's yeast to 1000 mL of Carolina spring water. Next, 175 mL of the solution was poured into seed culture dishes. Then, 2-4 boiled wheat grain pellets were added to each culture dish.

The paramecia culture was made by adding10 boiled wheat seeds to 25x150 millimeter petri dishes filled with deionized (DI) water. Afterwards, 1/5th of one 7.5 grain standard brewer's yeast tablet and 10 mL of paramecia culture were added to each dish and stored at 28 °C. 10 mL of the paramecia culture was added to the seed cultures.

The master culture was set up by adding 1 L of Carolina spring water to 4-1 L Erlenmeyer flasks. 15 boiled wheat seeds, 45 mL of seed culture, and 1 protozoa pellet were also added. The cultures were incubated at 28 °C.

**Brine Shrimp Culture**

Brine shrimp eggs (Brine shrimp direct, 80% Grade A, brine shrimp egg, Great salt lake origine) were refrigerated below 10°C before culture use. First, 15 g of sea salt (Instant Ocean) was added to 500 mL of DI water. The salt solution was poured into a brine shrimp hatchery dish (Hobby) to the fill line. Lastly, 1-3 0.4 g spoon-fools, provided by the hatchery kit, of brine shrimp eggs were added along the outer edge of the dish and the lid was added to the dish. The brine shrimp were kept at approximately 25°C. The brine shrimp hatched in 36-48 hours. After the incubation period, the sieve of the hatchery was removed, and the brine shrimp inside were rinsed with DI water to remove the salt.

**Oxygen Consumption Measurements**

The oxygen consumption measurements were collected at Day 5, 10, 15, and 20 of exposure. The measurements were collected using an optical oxygen sensor placed in a sealed 2 mL amber vial and automated intermittent respirometry software (AutoResp™). The oxygen was measured in $mgO_2/L/min$. To prepare for the measurements, the oxygen probe was calibrated using 10% sodium sulfite as the low oxygen measurement and aerated filtered system water as the high oxygen measurement. One fish was removed from the culture and a wet weight was

obtained. The fish was placed in the amber vial containing the aerated filtered system water, and the amber vial was placed in a 28°C water bath. To begin, the fish was acclimated for 10 min. Once a slight drop in oxygen measurements was displayed on the oxygen measurement graph the measurement was recorded as high oxygen level at time zero. After 30 minutes the displayed measurement was recorded as the low oxygen level. Blank measurements were obtained using aerated filtered system water.

The data was used to calculate the oxygen consumption rate. The low value was subtracted from the high value to represent the oxygen consumption rate. The oxygen consumption rate of the blanks was subtracted from the oxygen consumption rate of the zebrafish. The values were converted to mg$O_2$/kg/min. A paired sample t-test was performed between the SC fish and the treatment fish at each time point.

**RNA Extraction and RNA Sequencing**

Whole-genome transcriptomics, or RNA-sequencing (RNA-seq), analysis was also performed on embryo-larval zebrafish sub-sampled on Day 5 and 20 of exposure. Total RNA was extracted from whole fish using the NucleoSpin RNA extraction Kit from Clontech (Cat# 740902.5). Briefly, a whole-body homogenate was prepared by pooling 5 zebrafish per treatment in a lysis buffer. The sample was homogenized using a Pellet Pestle Motor. The lysate was then eluted through proprietary filters to retain RNA and wash DNA and other contaminating polymers (such as proteins). The extracted RNA was eluted using RNase-free $H_2O$, after which the concentration of RNA was quantified using a spectrophotometer. Once quantified, the RNA was stored at -80°C until RNA sequencing analysis. RNA-sequencing was performed by the Genomics and Bioinformatics Services at Texas A&M's AgriLife Research facility. An Illumina TruSeq sequencer was used to perform paired-end reads. The resulting sequenced files were

aligned to a zebrafish genome and associated transcript counts were determined by kind assistance from Dr. Xiaoning Qian at the Department of Electrical and Computer Engineering (ECE), Texas A&M University.

# CHAPTER III

# RESULTS

## Zebrafish Husbandry

The CPI-613 treatment group experienced mortality beginning at Day 7 of exposure and ceasing at Day 17 of exposure. The treatment group experienced a 29% loss. The SC group mortality began at Day 6 of exposure and ceased at Day 14 of exposure. The SC group experienced a 33% loss. The average fish weight for the SC group was 0.006 g. The average fish weight for the treatment group was 0.009 g (Figure 2). The nitrate, nitrite, and ammonia levels remained at 0 mg/L for both groups, and pH levels were between 7.40 and 8.07. Hardness measured at 150 mg/L. Salinity, conductivity, and temperature recorded a range of 0.34-0.344 g/L, 682-687 μS, and 27.0-28.6 °C respectively. The mean value for CPI-613 in the water over the 20 days of exposure between the two trials was 0.4 μM. The values on average were 40% of what they should have been.

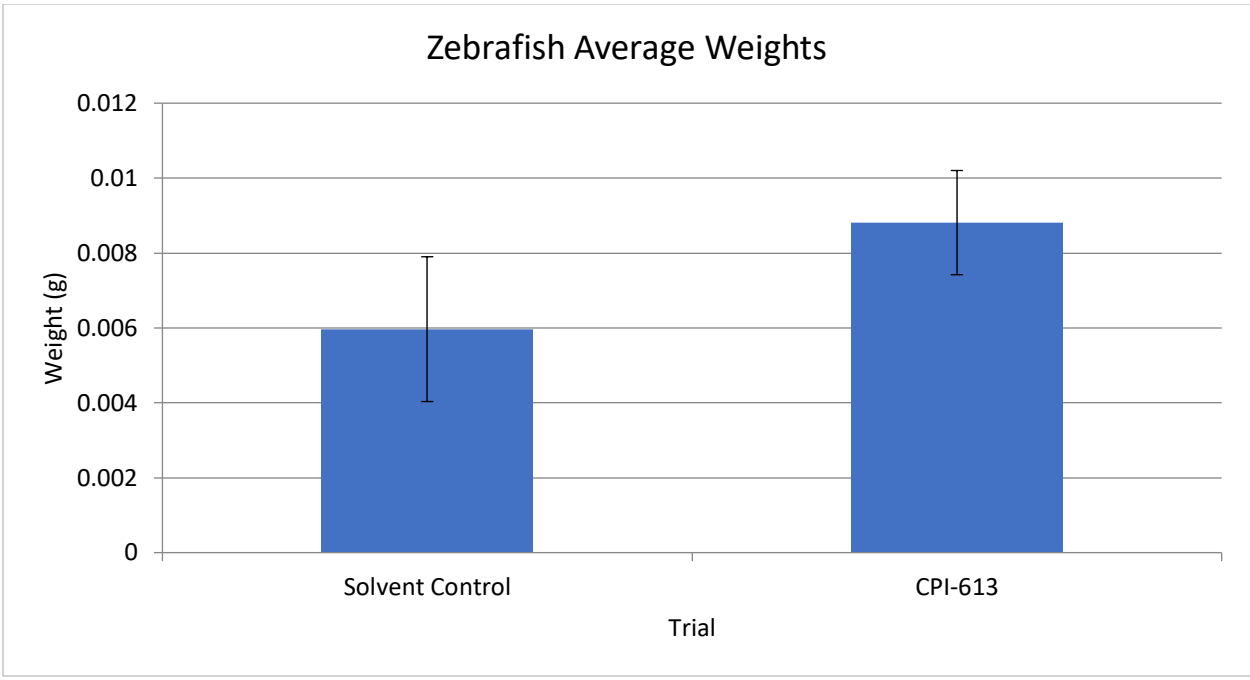


Figure 2. Average zebrafish weights of the solvent control and CPI-613 groups from Day 5 to 20 of exposure.

**Oxygen Consumption Measurements**

Both the treatment group and the SC group experienced an increase in oxygen consumption rate between Day 5 and 20 of exposure. The SC group experienced a 19.9% increase in oxygen consumption rate from Day 5 to 20 of exposure with an average standard error of 5.03 mgO2/kg/min. The treatment group experienced a 748% increase in oxygen consumption rate from Day 5 to 20 of exposure with an average standard error of 4.19 mgO2/kg/min. The overall trend of the oxygen consumption rate is illustrated in Figure 3.

At Day 5 of exposure, the treatment group oxygen consumption rate was significantly lower than the SC group ($t$=0.02 ($P$=0.05)). At Day 5 of exposure the SC group had an oxygen consumption rate of 16.83 ±3.92 mgO2/kg/min, and the treatment group had an oxygen

consumption rate of 3.67 ±1.73 mgO2/kg/min. The difference in oxygen consumption rate between the treatment group and the SC group at Day 5 of exposure was 13.17 mgO2/kg/min.

At Day 10 of exposure the treatment group oxygen consumption rate was still lower than the SC group oxygen consumption rate. The oxygen consumption rate of the treatment group was 8.83 ±4.21 mgO2/kg/min. The oxygen consumption rate of the SC group was 16.83 ±6.55 mgO2/kg/min. The difference in oxygen consumption rate between the treatment and SC groups at Day 10 of exposure was 8.00 mgO2/kg/min.

At Day 15 of exposure the oxygen consumption rate of the CPI-613 group surpassed the oxygen consumption rate of the solvent control group. The treatment group had an oxygen consumption rate of 20.04 ±5.92 mgO2/kg/min. The SC group had an oxygen consumption rate of 15.21 ±4.97 mgO2/kg/min. The difference in oxygen consumption rates between the treatment and SC groups at Day 15 of exposure was 4.84 mgO2/kg/min.

At Day 20 of exposure the treatment group had an oxygen consumption rate of 31.08 ±4.90 mgO2/kg/min. The SC group had an oxygen consumption rate of 20.18 ±4.69 mgO2/kg/min. The difference in oxygen consumption rates between the treatment and SC groups at Day 20 of exposure was 10.90 mgO2/kg/min.

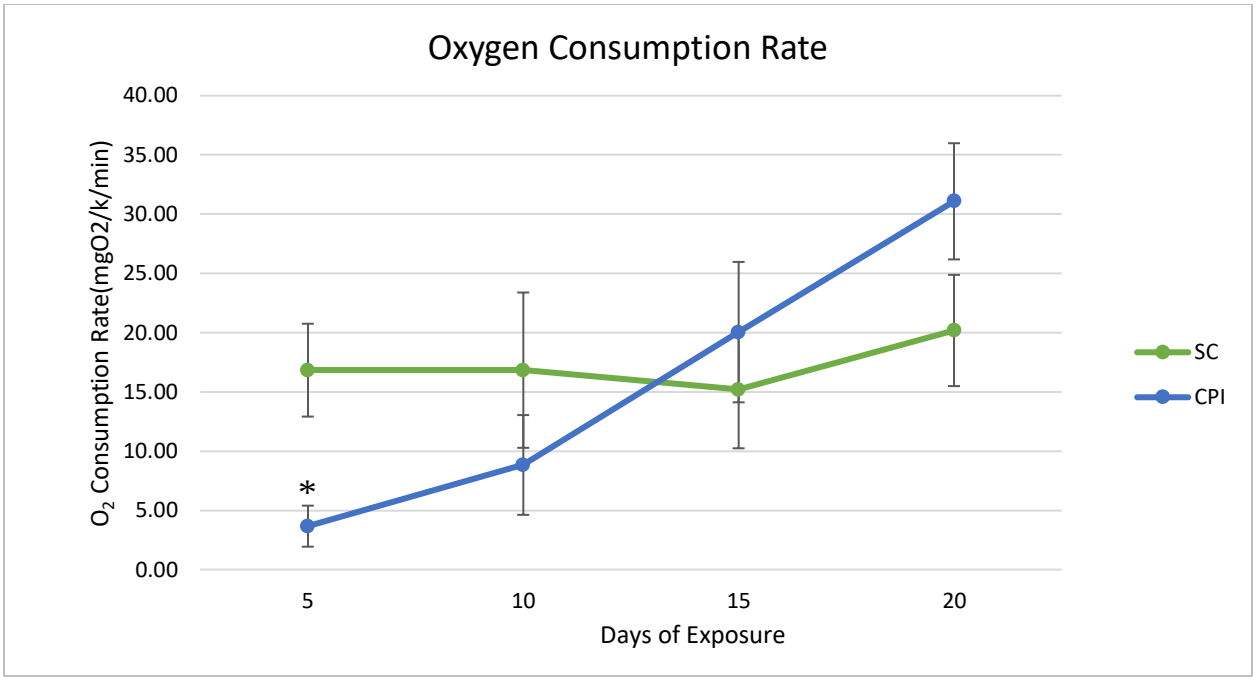


Figure 3. Rate of oxygen consumption measured at Day 5, 10, 15, and 20 of exposure. A statistically significant decrease in respiration rate was measured for the CPI-613 exposed group at Day 5 of exposure.

**RNA Sequencing Analysis**

RNA was extracted from treatment fish on Day 5 and 20 of exposure for RNA-seq analysis. The RNA was sequenced and quantified. Gene counts of zebrafish genes were analyzed for significant upregulations and downregulations of specific metabolic genes. The metabolic genes included those encoding for PDHC and HIF-1α.

The genes coding for PDHC were downregulated. The RNA counts for genes coding for PDHC at Day 5 and 20 were averaged. The downregulation for the PDHC genes were not significant based on the RNA counts for PDHC comparison on Day 5 and 20 of exposure (Figure 4). At Day 5 of exposure the average RNA count was 2517. At Day 20 of exposure the average

RNA count was 2144. The genes that coded for PDHC were pdha1a, pdhb, dlat, and pdhx. Pdha1b was an outlier and was excluded from the calculations.

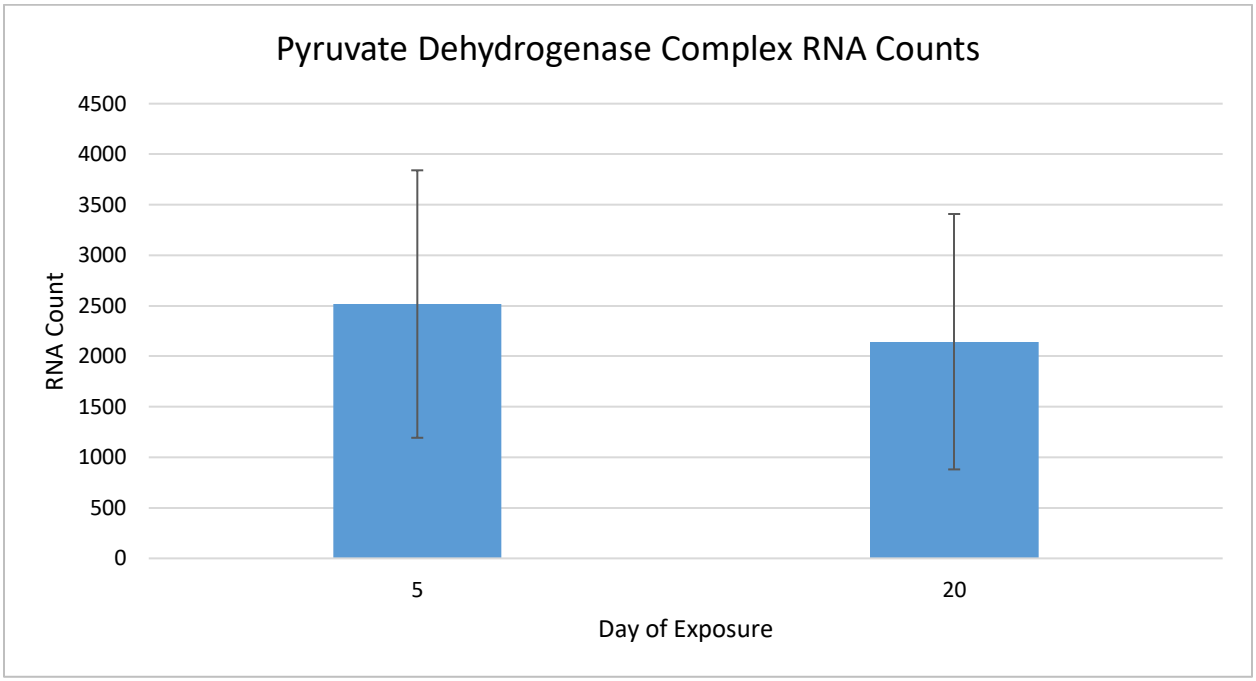


Figure 4. RNA counts of pyruvate dehydrogenase complex genes at Day 5 and 20 of exposure.

The genes coding for HIF-1 complex were also downregulated from Day 5 to 20 of exposure. Five HIF-1α genes were found in the sequence RNA, however three of the genes were outliers and were excluded from the calculations. The RNA counts of hif1ab and hif1al were averaged. The genes were down regulated significantly ($t$=0.007 ($P$=0.05)). At Day 5 of exposure, the average RNA count was 4711. At Day 20 of exposure the average RNA count was 2019 (Figure 5).

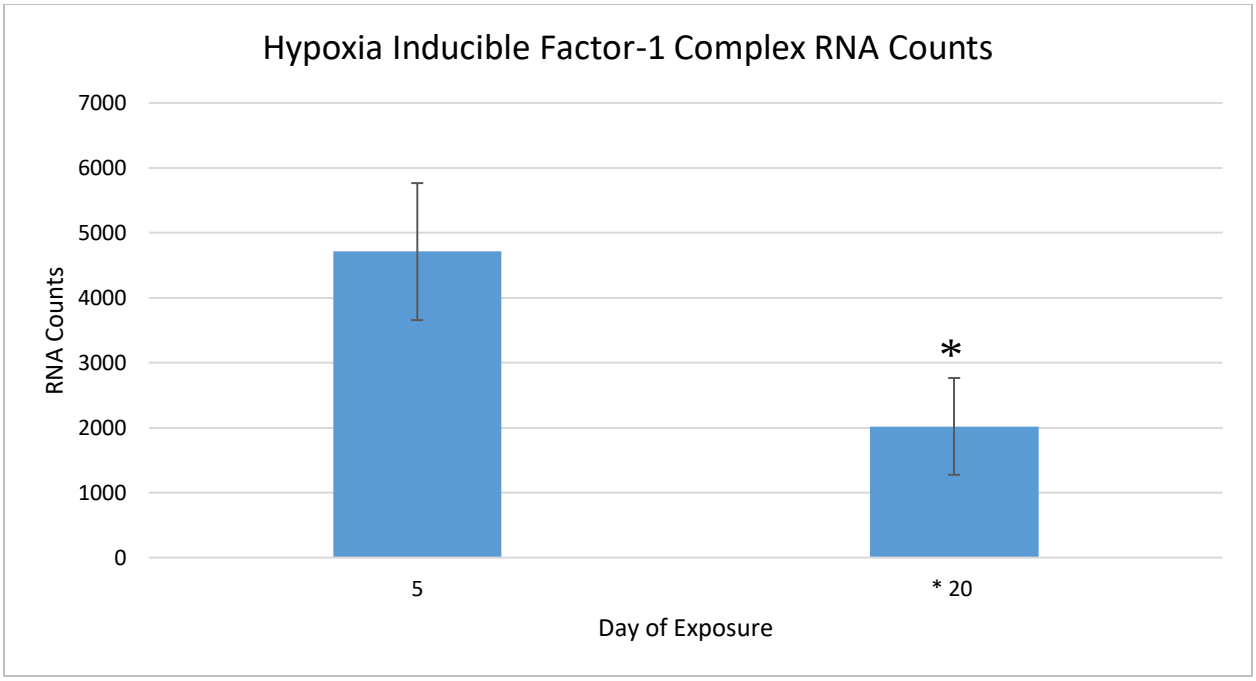


Figure 5. Hypoxia Inducible Factor-1 Complex RNA counts at Day 5 and 20 of exposure. Day 20 was significantly lower than Day 5 ($t$=0.007 ($P$=0.05)).

# CHAPTER IV

# CONCLUSION

In this study, I tested the effects of the metabolic disruptor CPI-613. I saw effects at both the physiological and molecular level. At the physiological level, the oxygen consumption rate of the zebrafish drastically decreased and then recovered by the end of the trial. At the molecular level I saw an induction of HIF-1α activity on the same day there was a decrease in respiration rate. However, there is no evidence from the RNA-seq data that CPI-613 targeted PDHC. There was no significant change in expression throughout the 20-day trial. Therefore, the zebrafish were affected, and they did recover, but the mechanism of the effect remains unclear.

Respiration rate is indicative to metabolic rate, which is used to represent overall physiological fitness. Therefore, there is compelling evidence that CPI-613 has an effect on zebrafish at the physiological level. This is evidently revealed as the initial decrease in respiration rate. At Day 5 of exposure the treatment group took in less oxygen. By Day 15, the treatment group had fully recovered. I conclude that there was a recovery from the effects of CPI-613 because the oxygen consumption rate of the treatment group reached the level of the oxygen consumption rate of the SC group. By Day 20 of exposure, the oxygen consumption rate of the treatment group exceeded the oxygen consumption rate of the SC group. This leads me to conclude that the zebrafish overcompensated for the effects of CPI-613 by some metabolic mechanism.

The effects of CPI-613 at the molecular level compliment the effects at the physiological level. At Day 5 of exposure, HIF-1α genes were expressed. By Day 20 of exposure, HIF-1α genes were significantly downregulated, which indicates that the HIF-1 complex was most active

on Day 5 of exposure. The downregulation of HIF-1α genes correlates with the increase in oxygen consumption rate of the zebrafish. From the respiration rate data, I conclude that the zebrafish were oxygen deprived at 5 Days of exposure and then recovered by Day 20 of exposure. It is logical that HIF-1α genes were expressed at a higher rate at Day 5 than Day 20 because HIF-1α is expressed to protect an organism from low oxygen stress. The transcription factor functions by controlling aerobic processes in order to maintain cellular homeostasis, which explains why the HIF-1α genes were upregulated at Day 5 of exposure when the zebrafish were the most stressed.

The CPI-613 target enzyme, PDHC, did not respond in the way that was expected. CPI-613 alters metabolism by inhibiting PDH, thus targeting the TCA cycle. PDHC was expected to be downregulated during exposure to CPI-613 due to this inhibition. Instead there was no observable change in PDHC gene expressions. It is possible that 1 μM of CPI-613 was not a high enough level to induce an effect on these genes. However, evidence (i.e. oxygen respiration rate and HIF-1α gene expression) indicates that CPI-613 does effect some mechanism of metabolism in zebrafish. Therefore, the mechanism that caused the decrease in oxygen consumption is unknown.

The goal of this study was to cause targeted metabolic disruption in zebrafish using CPI-613, and identify how zebrafish are effected by analyzing the organism at the physiological level as well as the molecular level. These affects were an indication of metabolic stress and adaptation. The zebrafish recovered their metabolic rate by activating HIF-1α, a transcription factor that is involved in coping with low oxygen stress. The target enzymes for CPI-613 were not evidently effected. It is unclear what mechanism was effected by CPI-613 to cause an effect on the zebrafish, but this is something that will be investigated further. 32,520 zebrafish genes

were sequenced, and this paper only analyzes six. My next step in the pursuit of this project is to investigate all of these genes to discover which ones might be driving the effects that are shown in this study. Therefore, the mechanism that caused the drop in oxygen consumption rate is still unknown and will be explored further.

# REFERENCES


Adeva, M., González-Lucán, M., Seco, M., and Donapetry, C., 2013. Enzymes involved in l-lactate metabolism in humans. Mitochondrion 13(6), 615-29.

Anderson, N.M., Mucka, P., Kern, J.G., and Feng, H., 2018. The emerging role and targetability of the TCA cycle in cancer metabolism. Protein Cell 9, 216–37.

Avdesh, A., Chen, M., Martin-Iverson, M. T., Mondal, A., Ong, D., Rainey-Smith, S., Taddei, K., Lardelli, M., Groth, D. M., Verdile, G., and Martins, R. N., 2012. Regular Care and Maintenance of a Zebrafish (*Danio rerio*) Laboratory: An Introduction. J Vis Exp (69), e4196.

Barabasi, A.L., and Oltvai, Z.N., 2004. Network biology: understanding the cell's functional organization. Nat Rev Genet 5, 101-13.

Bellio, C., DiGloria, C., Spriggs, D.R., Foster, R., Growdon, W.B., and Rueda, B.R., 2019. The Metabolic Inhibitor CPI-613 Negates Treatment Enrichment of Ovarian Cancer Stem Cells. Cancers 11, 1678-98.

Bolaños, J. P., Almeida, A., and Moncada, S., 2010. Glycolysis: A bioenergetic or a survival pathway? Trends Biochem. Sci 35(3), 145-9.

Burgard, A.P., and Maranas, C.D., 2003. Optimization-based framework for inferring and testing hypothesized metabolic objective functions. Biotechnol Bioeng 82, 670-7.

Ciccarone, F., Vegliante, R., Di Leo, L., and Ciriolo, M. R., 2017. The TCA cycle as a bridge between oncometabolism and DNA transactions in cancer. Semin Cancer Biol 47, 50-6.

Cline, A. J., Hamilton, S. L., and Logan, C. A., 2020. Effects of multiple climate change stressors on gene expression in blue rockfish (*sebastes mystinus*). Comp Biochem Phys 239(2020), 110580.

Cogliati, S., Lorenzi, I., Rigoni, G., Caicci, F., and Soriano, M. E., 2018. Regulation of mitochondrial electron transport chain assembly. J Mol Biol 430(24), 4849-73.

Dahlhoff, E.P., 2004. Biochemical indicators of stress and metabolism: applications for marine ecological studies. Annu Rev Physiol 66, 183-207.

Egawa, Y., Saigo, C., Kito, Y., Moriki, T., and Takeuchi, T., 2018. Therapeutic potential of CPI-613 for targeting tumorous mitochondrial energy metabolism and inhibiting autophagy in clear cell sarcoma. PLoS One 13(6), e0198940.

Eguchi, K., and Nakayama, K., 2019. Prolonged hypoxia decreases nuclear pyruvate dehydrogenase complex and regulates the gene expression. Biochem Biophys Res Commun 520(1), 128-35.

Enderle, J. D., 2012. Cellular respiration: Glucose metabolism and the creation of ATP. In J. Bronzino (Ed.), Introduction to biomedical engineering. Massachusetts: Academic Press 3, 485.

Evans, R. D., and Heather, L. C., 2019. Human metabolism: Pathways and clinical aspects. Surg 37(6), 302-9.

Fernández-García, J., Altea-Manzano, P., Pranzini, E., and Fendt, S., 2020. Stable isotopes for tracing mammalian-cell metabolism In Vivo. Trends Biochem Sci 45(3), 185-201.

Fernie, A. R., Carrari, F., and Sweetlove, L. J., 2004. Respiratory metabolism: Glycolysis, the TCA cycle and mitochondrial electron transport. Curr Opin Plant Biol 7(3), 254-61.

Fournier-Level, A., Perry, E. O., Wang, J. A., Braun, P. T., Migneault, A., Cooper, M. D., Metcalf, C. J., and Schmitt, J., 2016. Predicting the evolutionary dynamics of seasonal adaptation to novel climates in arabidopsis thaliana. Proc Natl Acad Sci 113(20), 2812-21.

Frazier, M.E., Johnson, G.M., Thomassen, D.G., Oliver, C.E., and Patrinos, A., 2003. Realizing the potential of the genome revolution: the genomes to life program. Science 300, 290-3.

Gobler, J. C., and Baumann, H., 2016. Hypoxia and acidification in ocean ecosystems: coupled dynamics and effects on marine life. Biol Lett 12, 20150976.

Gomez Isaza, D. F., Cramp, R. L., and Franklin, C. E., 2020. Living in polluted waters: A meta-analysis of the effects of nitrate and interactions with other environmental stressors on freshwater taxa. Environ Pollut 261, 114091.

Grasmann, G., Smolle, E., Olschewski, H., and Leithner, K., 2019. Gluconeogenesis in cancer cells – repurposing of a starvation-induced metabolic pathway? BBA-Rev Cancer 1872(1), 24-36.

Hackley, R. K., and Schmid, A. K., 2019. Global transcriptional programs in archaea share features with the eukaryotic environmental stress response. J Mol Biol 431(20), 4147-66.

Haggard, D.E., Noyes, P.D., Waters, K.M., and Tanguay, R.L., 2016. Phenotypically anchored transcriptome profiling of developmental exposure to the antimicrobial agent, triclosan, reveals hepatotoxicity in embryonic zebrafish. Toxicol Appl Pharmacol 308, 32-45.

Halpern, B.S., Walbridge, S., Selkoe, K.A., Kappel, C.V., Micheli, F., D'Agrosa, C., Bruno, J.F., Casey, K.S., Ebert, C., Fox, H.E., Fujita, R., Heinemann, D., Lenihan, H.S., Madin, E.M.P., Perry, M.T., Selig, E.R., Spalding, M., Steneck, R., and Watson, R., 2008. A Global Map of Human Impact on Marine Ecosystems. Science 319, 948-52.

Hartwell, L.H., Hopfield, J.J., Leibler, S., and Murray, A.W., 1999. From molecular to modular cell biology. Nature 402, C47-52.

Helfman, G.S., Collette, B.B., Facey, D.E., and Bowen, B.W., 2009. Chapter 1 - The Science of Ichthyology, The Diversity of Fishes - Biology, Evolution, and Ecology. pp. 3-10.

Helfman, G.S., Collette, B.B., Facey, D.E., and Bowen, B.W., 2009. Chapter 5 – Oxygen, metabolism, and energetics, The Diversity of Fishes - Biology, Evolution, and Ecology. pp. 57-74.

Hood, L., Heath, J.R., Phelps, M.E., and Lin, B., 2004. Systems biology and new technologies enable predictive and preventative medicine. Science 306, 640-3.

Jacob, E., Drexel, M., Schwerte, T., and Pelster, B., 2002. Influence of hypoxia and of hypoxemia on the development of cardiac activity in zebrafish larvae. Am J Physiol Regul Integr Comp Physiol 283(4), 911-7.

Jha, M. K., Lee, I., and Suk, K., 2016. Metabolic reprogramming by the pyruvate dehydrogenase kinase–lactic acid axis: Linking metabolism and diverse neuropathophysiologies. Neurosci Biobehav Rev 68, 1-19.

Jiang, B., 2017. Aerobic glycolysis and high level of lactate in cancer metabolism and microenvironment. Gen Dis 4(1), 25-7.

Kopperschläger, G., and Kirchberger, J., 1996. Methods for the separation of lactate dehydrogenases and clinical significance of the enzyme. J Chromatogr B Biomed Sci Appl 684(1-2), 25-49.

Kwong, R. W. M., Kumai, Y., Tzaneva, V., Azzi, E., Hochhold, N., Robertson, C. P., Bernd, and Perry, S. F., 2016. Inhibition of calcium uptake during hypoxia in developing zebrafish is mediated by hypoxia-inducible factor. J Ex. Biol 219(24), 3988-95.

Lee, K.C., Maturo, C., Perera, C.N., Luddy, J., Rodriguez, R., and Shorr, R., 2014. Translational assessment of mitochondrial dysfunction of pancreatic cancer from in vitro gene microarray and animal efficacy studies, to early clinical studies, via the novel tumor-specific anti-mitochondrial agent, CPI-613. Ann Transl Med 2(9), 91-101.

Locasale, J. W., 2018. New concepts in feedback regulation of glucose metabolism. Curr Opin Cell Biol 8, 32-8.

Lycan, T.W., Pardee, T.S., Petty, W.J., Bonomi, M., Alistar, A., Lamar, Z.S., Isom, S., Chan, M.D., Miller, A.A., and Ruiz, J., 2016. A Phase II Clinical Trial of CPI-613 in Patients with Relapsed or Refractory Small Cell Lung Carcinoma. PLoS One 11(10), e0164244.

Maj, M. C., Cameron, J. M., and Robinson, B. H., 2006. Pyruvate dehydrogenase phosphatase deficiency: Orphan disease or an under-diagnosed condition? Mol Cell Endocrinol 249, 1-9.

Mulukutla, B. C., Yongky, A., Le, T., Mashek, D. G., and Hu, W., 2016. Regulation of glucose metabolism – A perspective from cell bioprocessing. Trends Biotechnol 34(8), 638-51.

Pardee, T.S., Lee, K., Luddy, J., Maturo, C., Rodriguez, R., Isom, S., Miller, L.D., Stadelman, K.M., Levitan, D., Hurd, D., Ellis, L.R., Harrelson, R., Manuel, M., Dralle, S., Lyerly, S., and Powell, B.L., 2014. A Phase I Study of the First-in-Class Antimitochondrial

Metabolism Agent, CPI-613, in Patients with Advanced Hematologic Malignancies. Clin Cancer Res 20(20), 5255–64.

Pardee, T.S., Anderson, R.G., Pladna, K.M, Isom, S., Ghiraldeli, L.P., Miller, L.D., Chou, J.W., Jin, G., Zhang, W., Ellis, L.R., Berenzon, D., Howard, D.S., Hurd, D.D., Manuel, M., Dralle, S., Lyerly, S., and Powell, B.L., 2018. A Phase I Study of CPI-613 in Combination with High-Dose Cytarabine and Mitoxantrone for Relapsed or Refractory Acute Myeloid Leukemia. Clin Cancer Res 24(9), 2060-73.

Schadt, E.E., Zhang, B., and Zhu, J., 2009. Advances in systems biology are enhancing our understanding of disease and moving us closer to novel disease treatments. Genetica 136, 259-269.

Smart, A.G., Amaral, L.A., and Ottino, J.M., 2008. Cascading failure and robustness in metabolic networks. Proc Natl Acad Sci U S A 105, 13223-8.

Sousa Fialho, M. d. L., Abd Jamil, A. H., Stannard, G. A., and Heather, L. C., 2019. Hypoxia-inducible factor 1 signalling, metabolism and its therapeutic potential in cardiovascular disease. Biochim Biophys Acta Mol Basis Dis 1865(4), 831-43.

Stuart, S.D., Schauble, A., Gupta, S., Kennedy, A.D., Keppler, B.R., Bingham, P.M., and Zachar, Z., 2014. A strategically designed small molecule attacks alpha-ketoglutarate dehydrogenase in tumor cells through a redox process. Cancer Metab 2, 4.

Veerappa, S., and McClure, J., 2020. Intermediary metabolism. Anaesth. Intensive Care Med 21(3), 162-7.

Vuoristo, K. S., Mars, A. E., Sanders, J. P. M., Eggink, G., and Weusthuis, R. A., 2016. Metabolic engineering of TCA cycle for production of chemicals. Trends Biotechnol 34(3), 191-7.

Zachar, Z., Marecek, J., Maturo, C., Gupta, S., Stuart, S.D., Howell, K., Schauble, A., Lem, J., Piramzadian, A., Karnik, S., Lee, K., Rodriguez, R., Shorr, R., and Bingham, P.M., 2011. Non-redox-active lipoate derivates disrupt cancer cell mitochondrial metabolism and are potent anticancer agents in vivo. J Mol Med 89**,** 1137-48.

Zimorski, V., Mentel, M., Tielens, A. G. M., and Martin, W. F., 2019. Energy metabolism in

anaerobic eukaryotes and earth's late oxygenation. Free Radic Biol Med 140, 279-94.